

Effect of deposition time on surface plasmon resonance and Maxwell-Garnett absorption in RF-magnetron sputtered carbon-nickel films

VALI DALOUJI*

Department of Physics, Malayer University, Malayer, Iran

In this work, carbon-nickel films were grown during four deposition times (50 s, 90 s, 180 s and 600 s) at room temperature on glass substrates by radio frequency magnetron sputtering. The optical absorption spectra of the films were investigated with a special emphasis on the surface plasmon resonance (SPR) of Ni nanoparticles. The optical absorption peaks caused by the surface plasmon resonance of Ni nanoparticles were observed in the wavelength range of 300 nm to 330 nm. It has been shown that the surface plasmon resonance peaks exhibit a red shift and a blue shift depending on the deposition time. The red and blue shifts of the surface plasmon resonance in the absorption spectra of the films were observed with the increase and decrease of Ni nanoparticle size, respectively. The Ni nanoparticle size, dielectric function of carbon matrix ϵ_m and plasma frequency of free electrons ω_p for the films deposited at deposition time of 180 s have maximum values of 80 nm, 0.401 and $7.25 \times 10^{15} \text{ s}^{-1}$, respectively. These observations are in a good agreement with the electrical resistivity measurements and Maxwell-Garnett (M-G) effective medium theory (EMT).

Keywords: *surface plasmon resonance (SPR); carbon-nickel films; deposition time; deposition rate*

© Wroclaw University of Technology.

1. Introduction

Thin carbon-nickel films have many interesting properties which can be used in optic, electronic and coating technology [1–5]. The nonlinear optical properties of metal nanocomposite films have been widely investigated due to strong surface plasmon resonance (SPR) of metal nanoparticles in various dielectric matrixes, such as SiO_2 [6], Al_2O_3 [7], TiO_2 [8], NiO [9] and ZnO [10]. The SPR frequency is a significant characteristic parameter of the nonlinear optical properties which depends on content, size, and shape of metal nanoparticles, as well as the dielectric properties of metal particles and the surrounding matrix material [11]. Because of their interesting properties, the amorphous carbon a-C:Me (Me = Au, Ag, Cu, Mn. . .) have many applications as coating materials in biomedicine, electronics, mechanics and optics [12, 13]. The amorphous carbon-nickel

films, a-C:Ni, is characterized by distinct physical properties in comparison to carbide forming elements [14, 15]. In previous reports we studied the effects of deposition rate and annealing temperature on the morphology and the optical properties of carbon-nickel films [16–18]. In the present work we investigate the effect of deposition time on the surface plasmon resonance (SPR) peaks of carbon-nickel films.

2. Experimental

The carbon-nickel films have been prepared by RF-magnetron sputtering onto glass substrates using a mosaic target consisting of pure graphite and strips of pure nickel attached to the graphite. Before loading into the deposition chamber, the substrates were ultrasonically cleaned in acetone bath for 20 min and then dried in a hot air flow. The films were grown at room temperature in a deposition chamber evacuated to a base pressure of $5 \times 10^{-3} \text{ Pa}$ and then the constant Ar working

*E-mail: dalouji@yahoo.com

pressure of 4 Pa was settled and maintained by a throttle valve. Deposition of the films was done in a constant RF power regime at 400 W. The films were deposited at different deposition times: 50 s, 90 s, 180 s and 600 s. The thickness of the films was measured by Tencor Alpha Step 500 profiler. The field emission scanning electronic microscopy (FESEM) images were used for the morphological characterization. Energy dispersive X-ray studies (EDAX) were carried out with an AMETEK EDAX analyzer. The transmittance spectra were obtained by a double beam UV-Vis spectrometer in the range of 250 nm to 1000 nm (Jasco V-630). The direct current electrical conductivity was measured by cooling the samples in a continuous He flow in a cryogenic unit (optical low temperature model CCS 450 USA) of the thermostatic chamber in the temperature range of 15 K to 500 K. ORTEC (456, USA, 0 kV to 3 kV) high voltage power supply, Metrix VX102A (FRANCE) and Keithley 196 System DMM (USA) electrometers were used for voltage and current measurements, in temperature range of 15 K to 500 K.

3. Results and discussion

Fig. 1 shows the FESEM images of C–Ni films deposited at different deposition times 50 s to 600 s. As shown in the FESEM images, the size of the nickel nanoparticles increases for the films deposited at the deposition times of 50 s, 90 s and 180 s, and at 180 s it achieves a maximum value of about 80 nm. The size of the nanoparticles decreases then to about 20 nm after 600 s deposition (Table 1). The images indicate that the Ni nanoparticles are approximately spherical and dispersed in the amorphous carbon. Fig. 1e and Fig. 1f show the size distributions of Ni nanoparticles of C–Ni films deposited at 180 s and 600 s.

Fig. 2a shows the EDAX spectrum for the films obtained in the deposition time of 600 s. This spectrum was recorded in a line scan mode and one may observe the presence of peaks characteristic of C, Ni and Si. Fig. 2b shows that the Ni content, computed from the EDAX analysis, increased from

42 at.% to 85 at.% with the increase of the deposition time from 50 s to 180 s, and then decreased to 56 at.% for the films deposited in 600 s.

Fig. 3 shows the experimental absorption spectra of the C–Ni films deposited at different deposition times from 50 s to 600 s as a function of incident light wavelength. All the films exhibit an absorption peak in the wavelength region of 300 nm to 330 nm due to the SPR of Ni particles [19]. The deposition rate causes the increase of Ni nanoparticles size and enhanced intensity of the absorption peaks. The increase of Ni content causes the increase of bulk-like behavior, which manifests itself in the red shift of the surface plasmon resonance from 298 nm to 316 nm. With increasing the deposition time from 180 s to 600 s, the bandwidth of the absorption peak is narrowed and weakened. The increase of the deposition time manifests itself in the blue shift from 316 nm to 308 nm. These characteristics may be due to increasing significance of the quantum size effect [20].

The dielectric function $\epsilon(\omega)$ of a bulk metal has to be modified, giving rise to a size dependent dielectric function $\epsilon(\omega, R)$:

$$\epsilon(\omega, R) = \epsilon^{bulk}(\omega) - \epsilon_D^{bulk}(\omega) + \epsilon_D(\omega, R) \quad (1)$$

where $\epsilon^{bulk}(\omega)$ describes the dielectric function of a bulk metal calculated from n and k , whose values are obtained experimentally. The second term in this equation denotes the Drude dielectric function of a free electron gas and the third term denotes the dielectric function of a nanoparticle with a radius R defined by equation:

$$\epsilon_D(\omega, R) = 1 - \omega_p^2 / (\omega^2 + i\Gamma(R)\omega) \quad (2)$$

where ω_p represents the plasma frequency of free electron. The damping constant Γ is described for metal nanosphers with diameters smaller than the electron mean free path:

$$\Gamma(R) = v_f(1/L + A/R) \quad (3)$$

where v_f is Fermi velocity, L is the mean free path, R is the nanoparticle radius, and A is a proportionality constant ($A = 1$ for isotropic electron scattering) [21]. In the quasi-static regime where

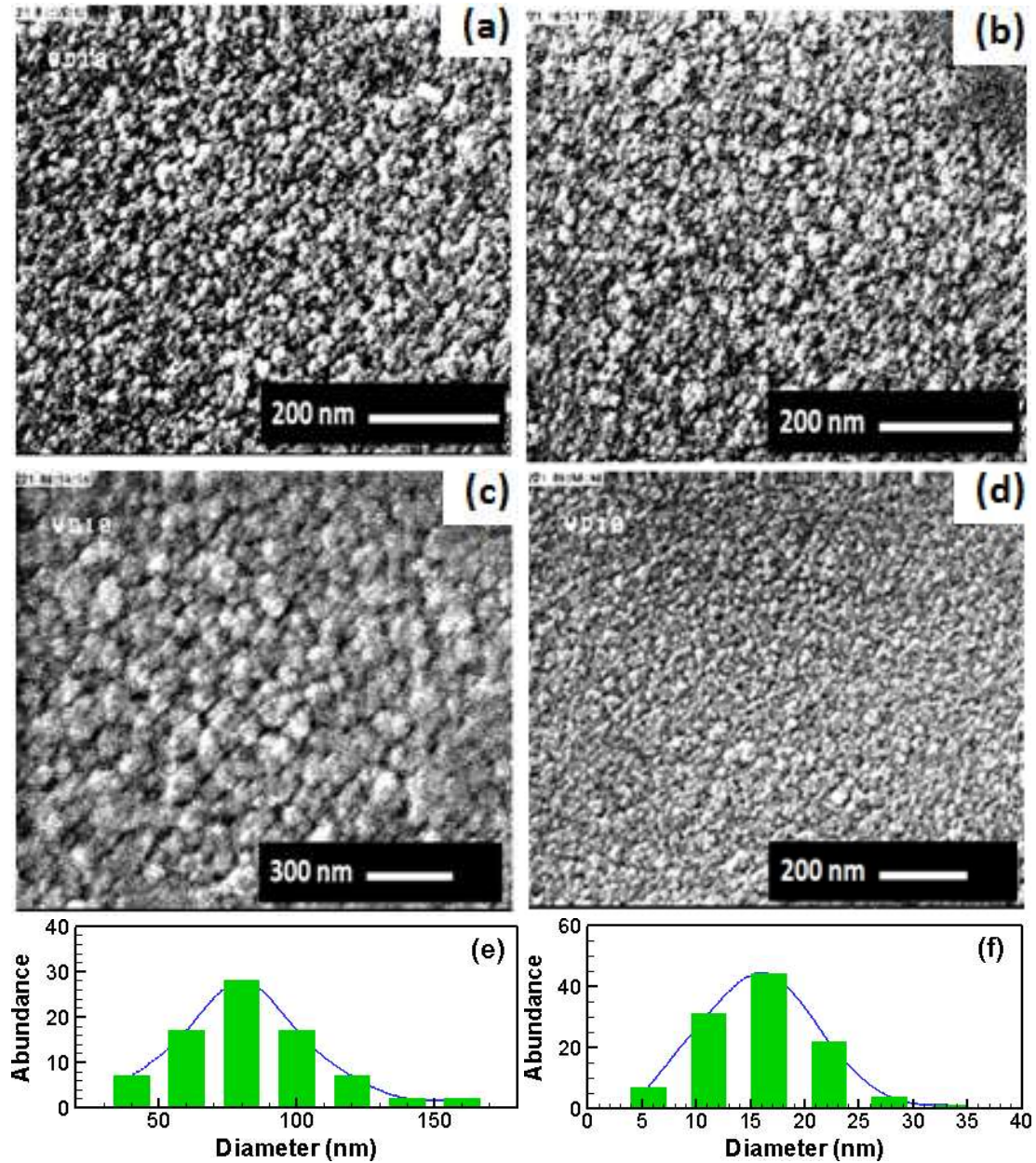


Fig. 1. FESEM images of C-Ni films deposited at deposition times of 50 s (a), 90 s (b), 180 s (c) and 600 s (d), and the size distribution of Ni nanoparticles of C-Ni films deposited at 180 s (e) and 600 s (f), respectively.

Table 1. Optical parameters of the C-Ni films deposited at different deposition times.

Deposition time [s]	Ni [at.%]	Ni nanoparticle size [nm]	ϵ_{bulk}	ϵ_{m}	$\omega_{\rho} \times 10^{15}$ [1/s]	$\nu_f \times 10^{17}$ [cm/s]
50	42	16.44	0.9991	0.05692	3.11	4.31
90	48	16.76	1.1848	0.09144	4.21	4.26
180	85	82.21	24.1889	0.40158	7.26	10.72
600	56	17.95	11.0576	0.13541	5.37	7.32

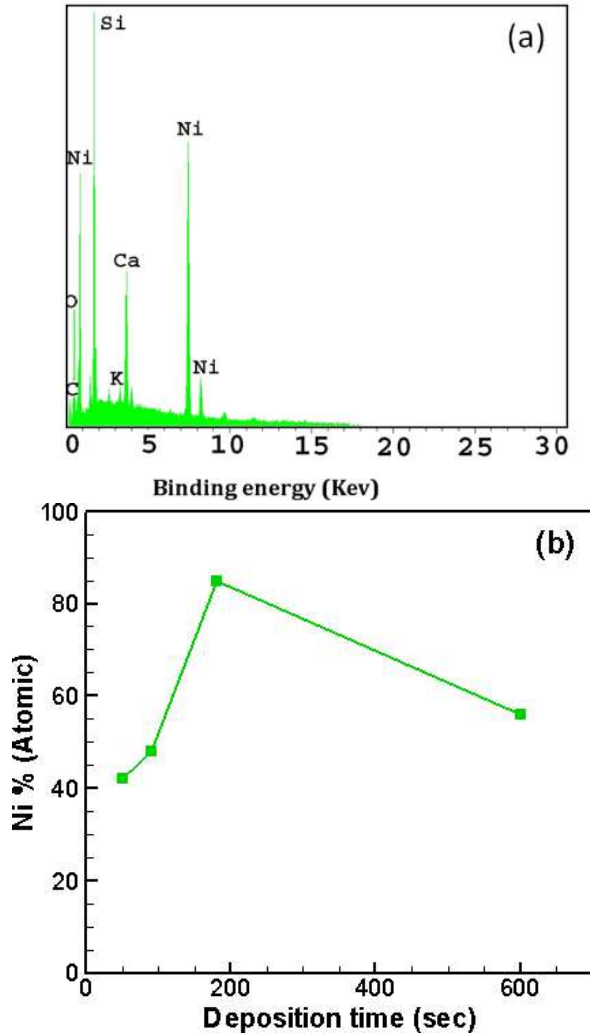


Fig. 2. EDAX spectrum of C–Ni film deposited at 600 s (a) and variation of Ni content with deposition time (b).

the radius R is significantly smaller than the incident wavelength λ , phase retardation and the mixing of higher-order multiple oscillations are negligible. In this case, a more simplified expression, based on the dipole approximation can be used, as given by [22]:

$$Q_{abs}(\omega) = 18\pi V \epsilon_m^{3/2} \epsilon_2(\omega) / \lambda [(\epsilon_1(\omega) + 2\epsilon_m)^2 + \epsilon_2(\omega)^2] \quad (4)$$

If $\epsilon_2(\omega)$ is small or slightly dependent on ω , the resonance condition in which the peak of the SPR band occurs is approximately fulfilled when

$\epsilon_1(\omega) = -2\epsilon_m$, where V is the volume fraction of metal, $\epsilon_1(\omega)$, $\epsilon_2(\omega)$ and ϵ_m are real and imaginary part of dielectric constant of the particles and dielectric constant of carbon matrix, respectively. The imaginary part of the particles dielectric constant is given as [22]:

$$\epsilon_2(\omega, R) = \epsilon_2^{bulk}(\omega) + 3\omega_p^2 v_f / 4\omega^3 R \quad (5)$$

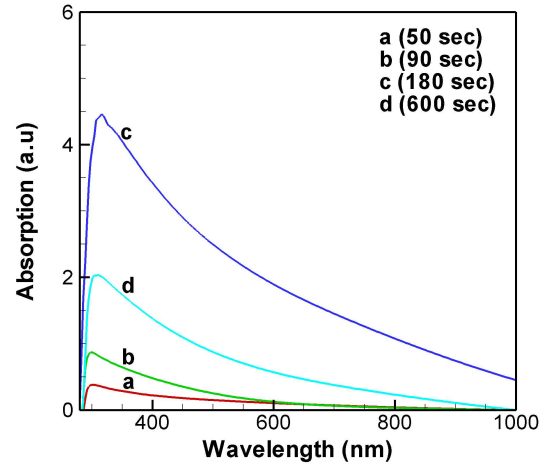


Fig. 3. The experimental absorption spectra of C–Ni films for the films deposited at different deposition times.

The enhanced nonlinear optical absorption properties of the C–Ni films deposited at the time up to 180 s could be attributed to the highly dispersed Ni nanoparticles whose size increases with its content. On the other hand, the weakening of the nonlinear optical absorption properties with further increase of the deposition time over 180 s, results from the decrease in Ni content. The SPR peak shows a red shift trend with increasing deposition time from 50 s to 180 s and then turns to blue shift from 180 s to 600 s. The red shift of the SPR peak in the films deposited in the time of 50 s to 180 s may be due to the quantum size effect. Besides the SPR shift there is the sharpening of the peak with increasing deposition time, which is attributed to the enhanced intrinsic free electron oscillation inside the metal particles. The broadening of the related SPR band may be due to the mean free path effect as well as the influence of conduction electron collisions with particle surfaces.

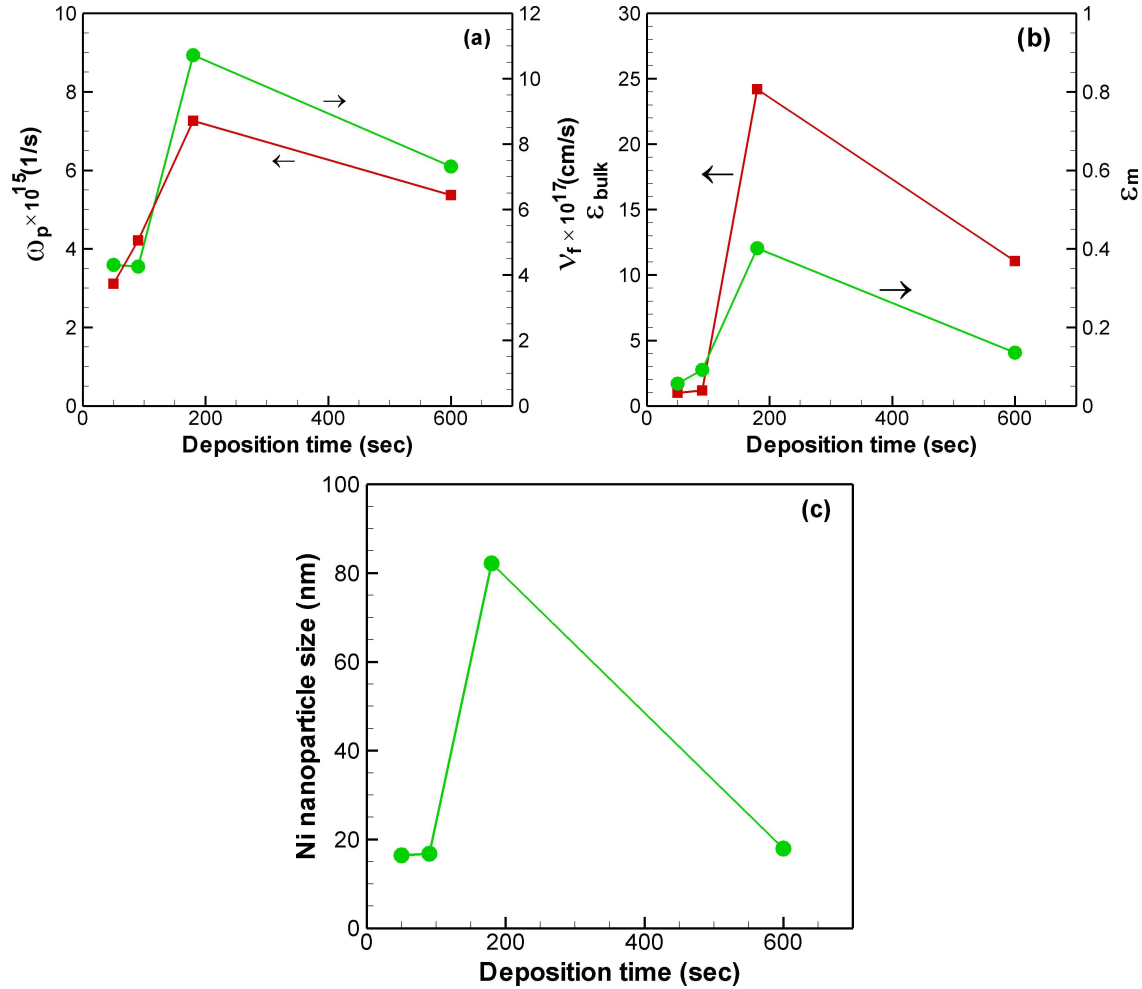


Fig. 4. Variation of ω_p and ν_f (a), $\epsilon^{bulk}(\omega)$ and ϵ_m , (b) and Ni nanoparticle size (c) of the C-Ni films with respect to the deposition time.

The blue shift accompanying the narrowing of the peak in the films deposited from 180 s to 600 s is related to decreasing in Ni content and Ni nanoparticle size. Therefore, the optical properties of the C-Ni films including the position and intensity of the absorption peak can be controlled by altering Ni content according to the requirement of a practical application. Fig. 4a shows the variation of ω_p and ν_f with respect to deposition time. It can be seen that due to the increase of free carrier concentration in the samples deposited up to 180 s, ω_p and ν_f increase and then, due to decreasing free carrier concentration in the samples deposited from 180 s to 600 s, they decrease. Fig. 4b shows the variation of $\epsilon^{bulk}(\omega)$ and ϵ_m with respect to the

deposition time. It can also be seen that due to increasing free carrier concentration in the samples obtained in the deposition times up to 180 s, $\epsilon^{bulk}(\omega)$ and ϵ_m increase and then decrease. Fig. 4c shows the variation of the Ni nanoparticle size with respect to deposition time. As shown in FESEM images, due to increasing deposition rate up to 180 s, the Ni nanoparticle size increases and then over 180 s, it decreases due to decreasing deposition rate. At the low deposition rate and high deposition time, there are some adsorbed atoms which have enough time to migrate to the sites where the surface energy is low enough to be covered by the coming atom and, as a result, the film surface is very smooth and has small particle size.

Therefore, the increase of deposition time causes changing of deposition mode, deposition rate and hence, strongly affects the size of the particles.

Fig. 5 shows the theoretical Maxwell-Garnett absorption spectra of C–Ni films with respect to wavelength. The plasmon resonant modes are described by Maxwell-Garnett model by introducing a shape-dependent factor $\kappa = 1/(q - 1)$ where q is the depolarization factor. The Maxwell-Garnett absorption theory can be written in terms of the particle polarizability α as:

$$Q_{abs} = k\text{Im}(\alpha)$$

and

$$\alpha = (V/3q)(\epsilon_m - \epsilon_p)/(\epsilon_m + \kappa\epsilon_p) \quad (6)$$

where k is the wave vector and V is the particle volume.

The optical absorption behavior of the films can be stated by Maxwell-Garnett (M-G) effective medium theory (EMT) and defined by [20]:

$$\epsilon_{eff} = \epsilon_m \left[\frac{(\epsilon_p + 2\epsilon_m + 2V(\epsilon_p - \epsilon_m))}{(\epsilon_p + 2\epsilon_m - 2V(\epsilon_p - \epsilon_m))} \right] \quad (7)$$

where ϵ_p , ϵ_m , ϵ_{eff} and V are the dielectric function of the particles, the dielectric function of the matrix, the effective dielectric function of the films and the volume fraction occupied by the spherical particles, respectively [23].

The absorption maximum occurs at a wavelength satisfying:

$$\epsilon_p + 2\epsilon_m - 2V(\epsilon_p - \epsilon_m) = 0 \quad (8)$$

It can be seen that with an increase of deposition time up to 180 s Maxwell-Garnett absorption spectra and the imaginary part of the effective dielectric constant ϵ_{eff} increase and then over 180 s they decrease. The increase in absorption spectra in the films deposited from 50 s to 180 s is due to the increase in the concentration of Ni atoms, whereas the decrease in the absorption spectra in the films deposited from 180 s to 600 s is due to the decrease in concentration of Ni atoms.

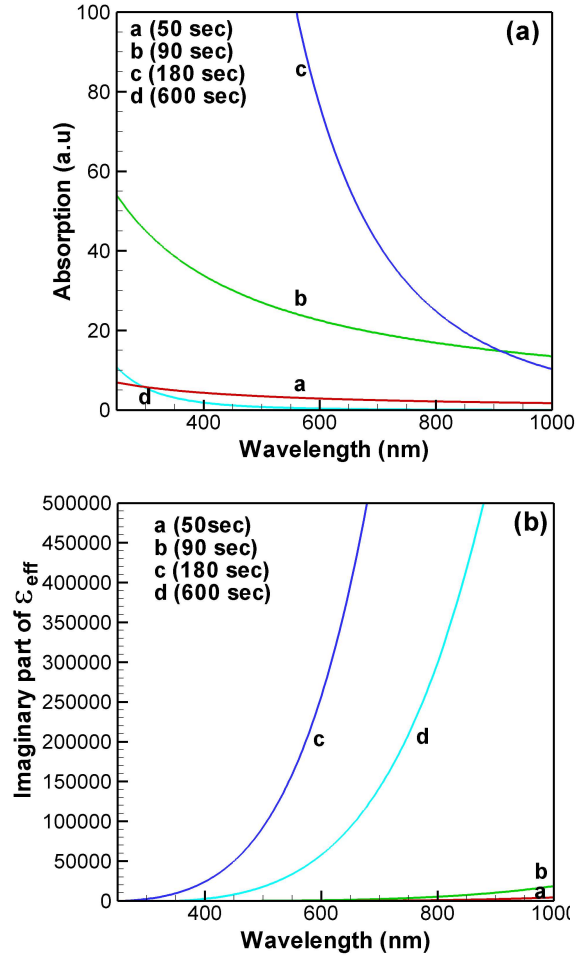


Fig. 5. The theoretical Maxwell-Garnett absorption spectra (a) and the imaginary part of the effective dielectric constant ϵ_{eff} (b) of C–Ni films for the films obtained at different deposition times.

Fig. 6 shows the variation of resistivity with temperature for the films deposited at different deposition times of 50 s to 600 s. The resistivity of the films decreases with increasing temperature showing the semiconducting behavior. It is evident that in the entire temperature range 15 K to 500 K, the resistivity decreases with increasing deposition time from 50 s to 180 s and then it increases for the deposition times from 180 s to 600 s. The decrease of resistivity could be due to the increase of nanoparticle size which leads to the decrease in grain boundary scattering. On the other hand, the increase of resistivity at the deposition time above

180 s may be due to the increase of grain boundary scattering.

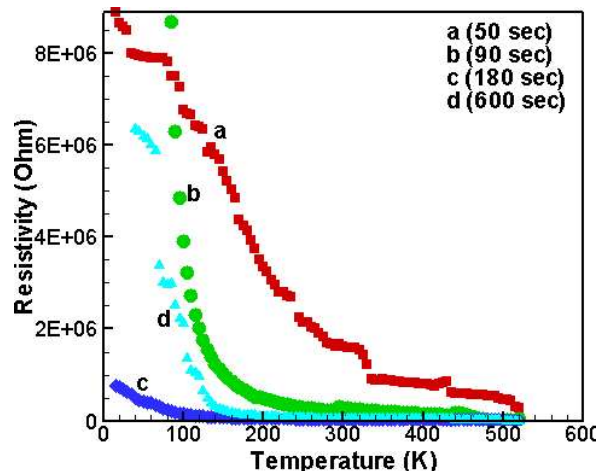


Fig. 6. Variation of resistivity with temperature for the films deposited for 50 s, 90 s, 180 s and 600 s.

4. Conclusions

In this study, we showed that deposition time and deposition rate play an important role in the optical properties of C–Ni films. It is observed that the films deposited in 180 s have maximum surface plasmon resonance peak intensity and nickel concentration. It can be seen that at 180 s ω_p , ν_f , $\epsilon^{\text{bulk}}(\omega)$, the size of Ni nanoparticles and the dielectric function matrix ϵ_m of the C–Ni films achieve maximum values and over 180 s they decrease.

References

- [1] TALU S., BRAMOWICZ M., KULESZA S., SHAFIKHANI A., GHADERI A., MASHAYEKHI F., SOLAYMANI S., *Ind. Eng. Chem. Res.*, 54 (2015), 8212.
- [2] STACH S., GARCZYK Z., TALU S., SOLAYMANI S., GHADERI A., MORADIAN R., NEZAFAT NEGIN B., ELAHI S.M., GHOLAMALI H., *J. Phys. Chem. C*, 119 (2015), 17887.
- [3] TALU S., STACH S., GHODSELAHI T., GHADERI A., SOLAYMANI S., BOOCHANI A., GARCZYK Z., *J. Phys. Chem. B*, 119 (2015), 5662.
- [4] TALU S., STACH S., SOLAYMANI S., MORADIAN R., GHADERI A., HANTEHZADEH M.R., ELAHI S.M., GARCZYK Z., IZADYAR S., *J. Electroanal. Chem.*, 749 (2015), 31.
- [5] GHODSELAHI T., VASEGHI M.A., SHAFIEKHANI A., *J. Phys. D Appl. Phys.*, 42 (2009), 015308.
- [6] SANGAPOUR P., AKHAVAN O., MOSHFEGH A.Z., *J. Alloy. Comp.*, 486 (2009) 22.
- [7] CELEP G., COTTAANCIN E., LERME J., PELLARINE M., ARNAUD L., HUNTZINGER J.R., VIALLE J.L., BROYER M., PALPANT B., BOISRON O., MELINON P., *Phys. Rev. B*, 70 (2004) 165409.
- [8] LIAO H.B., XIAO R.F., WONG H., WONG K.S., WONG G.K.L., *Appl. Phys. Lett.*, 72 (1998) 1817.
- [9] FERREIRA F.F., HADDAD P.S., FANTINI M.C.A., BRITO G.F.S., *Solid Stat Ionics*, 165 (2003), 0161.
- [10] LIAO H.B., WEN W.J., WONG G.K.L., YONG G.Z., *Opt. Lett.*, 28 (2003), 1790.
- [11] KREIBIG U., VOLLMER M., *Optical Properties of Metal Clusters*, Springer-Verlag, Berlin – Heidelberg – New York, 1995.
- [12] ENDRINO J.L., ESCOBAR GALINDO R., ZHANG H.S., ALLEN M., GAGO R., ESPINOSA A., ANDERS A., *Surf. Coat. Tech.*, 202 (2008), 3675.
- [13] GHODSELAHI T., VASEGHI M.A., SHAFIKHANI A., AHMADI M., PANAHADEH M., HEIDARI SAANI M., *Physica B*, 405 (2010), 3949.
- [14] KOROTCENKOV G., HAN S.D., STETTER J.R., *Chem. Rev.*, 109 (2009), 1402.
- [15] KAMBHAMPATI D.K., KNOLL W., *Curr. Opin. Colloid Interf. Sci.*, 4 (1999), 273.
- [16] ELAHI S.M., DALOUJI V., VALED-BAGI S., *Adv. Mater. Sci. Eng.*, 2013 (2013), 506549.
- [17] ELAHI S.M., DALOUJI V., MEHRPARVAR D., VALED-BAGI S., *Mol. Cryst. Liq. Cryst.*, 587 (2013), 105.
- [18] DALOUJI V., ELAHI S.M., *J. Korean Phys. Soc.*, 64 (2014), 857.
- [19] FOX M., *Optical Properties of Solids*, Oxford University Press Inc., New York, 2001.
- [20] WANG S.-J., ZHANG B.-P., YAN L.-P., DENG W., *J. Alloy. Comp.*, 509 (2011), 5731.
- [21] HASHIMOTO S., WERNER D., UWADA T., *J. Photoch. Photobiol. C*, 13 (2012), 28.
- [22] NADERI S., GHADERI A., SOLAYMANI S., GOLZAN M.M., *Eur. Phys. J. Appl. Phys.*, 58 (2012), 20401.
- [23] DALACU D., MARTINU L., *J. Appl. Phys.*, 87 (2000), 228.

Received 2015-07-25

Accepted 2016-03-11